

Hydrogen/deuterium exchange mass spectrometry and NMR uniquely reveal different aspects of dynamic allostery

Ganesh S. Anand¹, Riley B. Peacock² and Elizabeth A. Komives^{2,*}

¹Department of Chemistry, Pennsylvania State University, University Park, PA 16802, USA;

²Department of Chemistry & Biochemistry, University of California, San Diego, La Jolla, CA 92093-0378, USA.

ABSTRACT

NMR experiments probe protein dynamics across a broad range of time scales from nsec to sec and as such, NMR is the gold standard for discovering and analyzing dynamic allostery in proteins. The protein ensemble of states reconfigures upon ligand binding, and NMR alone can assess which residues have changed their motions and on what timescales. Amide hydrogen/deuterium exchange mass spectrometry (HDX-MS) also often reveals reconfiguration of the protein ensemble upon ligand binding, but the timescale of motions that are reflected in the HDX-MS experiment is more difficult to ascertain. A few allosteric proteins have now been studied by both NMR and HDX-MS allowing a direct comparison of the data from both methods revealing the complementarity of the results from these different experiments as well as information about the timescales of motion reflected in the HDX-MS results. The insights gained from comparing NMR and HDX-MS of small monomeric proteins enable a clearer interpretation of the allostery revealed by HDX-MS in larger protein complexes and assemblies that are not amenable to NMR.

KEYWORDS: protein dynamics, conformational heterogeneity.

INTRODUCTION

Allostery

Allostery is remarkably prevalent in regulating important biological processes and in signal transduction, and experimental observations of apparent allostery have increased markedly over the past 25 years. The concept of allostery in proteins was first formulated by several groups in the 1960s. The term allostery comes from the Ancient Greek *allos* (ἄλλος), “other”, and *stereos* (στερεός), “solid (object)”. The term was coined to emphasize the distinction between the regulatory site which is physically distinct from the active site. Early models of allostery focused on multimeric proteins. These include the pioneering concerted model put forth by Monod, Wyman, and Changeux (the MWC model) [1] and the sequential model described by Koshland, Nemethy, and Filmer (the KNF model) [2]. Both invoke a two-state conformational model in which, the relaxed (R) state binds substrate more readily than the tensed (T) state. These early models of allostery can now be understood as a subset of a broad range of phenomena in which binding at one site perturbs the conformational ensemble of the protein allowing changes in the binding thermodynamics at a second site.

In the current view of allostery, the protein is understood as an ensemble of conformational states which interconvert with small energy barriers of a few $k_B T$ of energy (eg 2-10 kcal/mol) (Figure 1),

*Corresponding author: ekomives@ucsd.edu

instead of a purely structural binary model of coupling between different sites. This view helps explain observations of allostery that occur without crystallographic evidence of structural changes, and reflects the fact that allostery can also occur in monomeric proteins [3, 4]. A theoretical framework that unites the various ways of looking at allostery including thermodynamics, free energy landscape of population shift, and structure that emphasizes the importance of communication between binding sites has been proposed [5].

The timescale of interconversion between the conformational substates will depend on the height of the energy barrier. Some substates, such as A and A' which interconvert by pathway 1 in Figure 1 cannot be resolved by some techniques or experimental conditions, because they interconvert rapidly (on the order of microseconds) and with a very low energy barrier. For example, experiments conducted at 25 °C, will measure the average of the A and A' states, as these states will both be populated. In contrast, states A and B interconvert more slowly because the energy barrier between them is higher. These states are more likely to be observed separately. The relative populations of state A and B depend on their energies according to Boltzmann's law. In allostery, ligand binding shifts the energies of state A and B such that B becomes the predominant state in the ligand-bound form. The energy landscape view helps diffuse the question of "induced fit" vs "conformational selection". As can be seen from the diagram, both states A and B exist, however one may be at such a low concentration due to its higher energy that it won't be observed until the ligand binds leading to the supposition of "induced fit". When both states are observed because their energies are not that different, or the experiment is sensitive enough to observe the lowly populated state, "conformational selection" will be invoked. Clearly these are two limits of the same physical phenomenon of altered energies of protein states upon ligand binding.

Besides understanding the energetics of allostery, it is also important to think about the "pathway" between the two binding sites. Newton's cradle helps visualize the process of allostery, and it emphasizes an important concept that will be brought out further in this review. In Newton's cradle, momentum and energy are largely conserved and

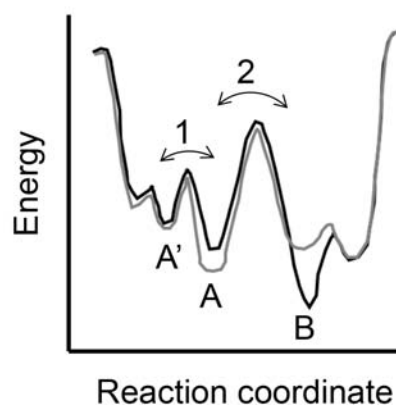


Figure 1. Energy landscape diagram showing two states, A and B that are separated by a large enough energy barrier that they will have different chemical shifts and can be observed separately. States A and A' are close in energy and though different, most experimental measurements, particularly at 25 °C, will measure the average between them.

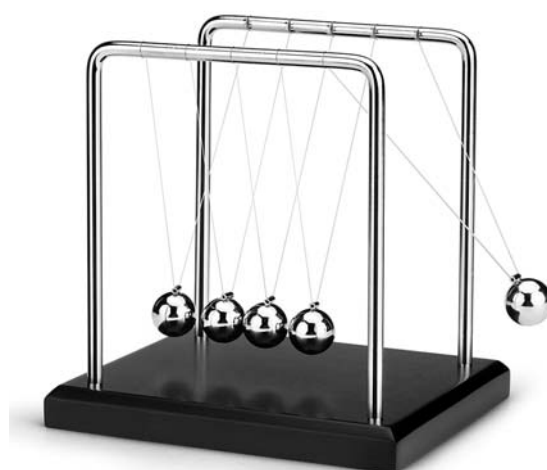


Figure 2. Newton's cradle helps us understand the conservation of momentum and energy with swinging spheres. When one of the end spheres strikes the stationary spheres, it transmits a force through the stationary spheres that pushes the last sphere out. This phenomenon is similar to what happens in allosteric proteins.

the ramifications of this conservation are that the middle spheres do not appear to move while the force is transmitted through them from one end to the other (Figure 2). Indeed, allostery would not occur through proteins if the thermodynamic force induced by ligand binding to the allosteric site

was dissipated through the interior of the protein structure before impacting the active site. We see this in an analysis of frustration in allosteric proteins. Frustration refers to whether an amino acid side chain is making preferred interactions or not. Generally, the core of folded proteins is minimally frustrated whereas highly frustrated residues occur in patches on the surface that correlate with allosteric sites [6] (Figure 3). Thus, a minimally-frustrated protein core is optimized for transducing an allosteric signal between highly frustrated sites. An analogy to soft matter has been made to describe hydrophobic core segments involved in allosteric propagation [7].

NMR reveals the timescale and populations of allosteric transitions

One of the earliest reports of dynamic allostery was from Mildvan's group in 1996 [8]. By performing ^{15}N relaxation studies of the enzyme 4-oxalocrotonate tautomerase both free and bound to the inhibitor, *cis,cis*-muconate, they were able to show that ps – ns motions decreased in seven backbone NH groups and increased in eight backbone NH groups upon inhibitor binding. Such ^{15}N relaxation experiments combined with heteronuclear nuclear Overhauser effects (NOEs) can be analyzed to obtain order parameters for the protein backbone. Motions on the ps-ns timescale are also readily predicted by conventional molecular dynamics simulations and the predicted order parameters from such simulations correlate well with order parameters measured by NMR [9]. In addition, regions with low order parameters were strongly correlated to regions containing

highly frustrated residues (Figure 4) [10]. In 4-oxalocrotonate tautomerase chemical exchange, reflecting μs -ms time scale motions, increased at the active site and at the subunit interface (far away from the inhibitor binding site) upon inhibitor binding. These authors pointed out that it is the μs -ms time scale motions that are likely to be linked to binding ($k_{\text{on}} \sim 10^6 \text{ M}^{-1} \text{ s}^{-1}$) and catalysis ($k_{\text{cat}} \sim 10^3 \text{ s}^{-1}$) [8]. Since this early report, NMR has become the gold standard experimental approach for studying allostery. It affords single residue resolution and allows for measurement of both backbone and

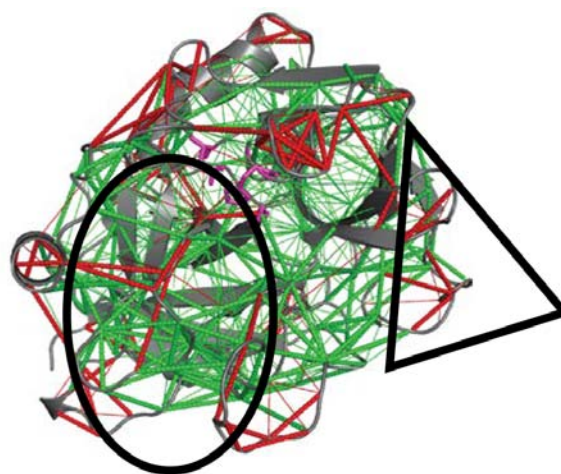


Figure 3. Frustratometer output for thrombin showing the minimally frustrated core of the protein (green lines indicate contacts that are energetically preferred) and highly frustrated surface patches (red lines indicate contacts that are energetically unfavorable). The triangle marks the allosteric site and the oval marks the active site.

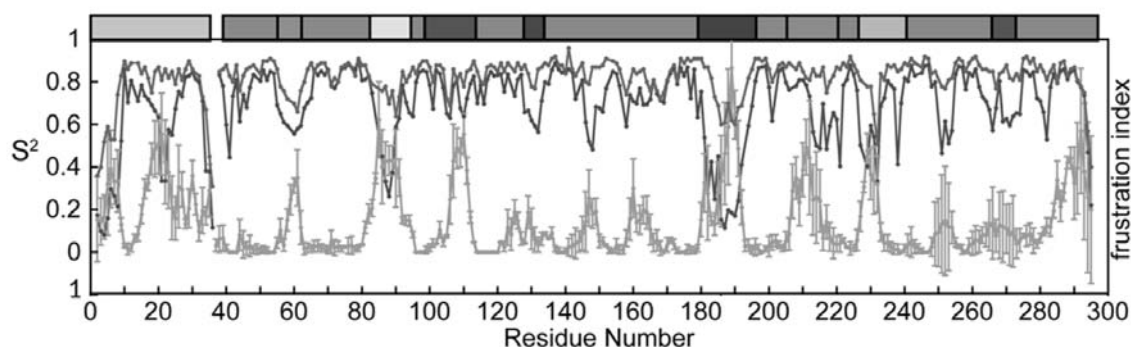


Figure 4. Comparison of residual frustration with NMR-derived order parameters shows a strong correlation indicating that mobile regions are likely to also contain frustrated residues. The bars above the graph mark the thrombin surface loops.

side chain motions. The general consensus now seems to be that ps-ns backbone motions usually do not reflect allostery, because these motions are too rapid.

Chemical exchange between the ground state and an “invisible state” or a low populated state occurs on the μ s-ms time scale and can be measured by Carr-Purcell-Meinboom and Gill-type (CPMG or relaxation dispersion) experiments [11]. In this experiment, backbone NH groups that are exchanging between states have broadened signals due to slightly different chemical shifts of the NH group in each state. By applying refocusing pulses, the rate of interconversion between the two states can be measured. In addition, the populations of each state can be ascertained. Typically, one state will be ~95% populated while the “invisible state” or the low populated state accounts for only 5%. It is impossible to cite all of the different proteins in which allostery has been observed using relaxation dispersion experiments, but we will point the reader to a few recent reviews [12-14].

Newer NMR methods monitor side chain methyl groups and also reveal hidden/higher energy conformational states. Kay’s group used methyl transverse relaxation-optimized spectroscopy (TROSY) NMR to study the cooperativity between catalytic sites and effector binding sites in aspartate transcarbamoylase, which has six catalytic and six regulatory subunits [15]. Although only the T state could be observed for the unliganded enzyme, clear signals were observed at different chemical shifts indicating population of the R state upon active site binding. Because ligand binding and the R–T equilibrium are linked, they were able to measure the equilibrium constant between unliganded R and T forms, despite the fact that the R state is “invisible”. This paper is well-worth reading as a beautiful description of how NMR can be used to measure the various equilibrium constants required for the MWC model of allostery. Two recent papers have used state-of-the-art NMR methods to show that kinases have more than one inactive state and how mutations and binding of various drugs and effectors shift the conformational equilibrium between these states [16, 17]. In the latter example, the experiment that is analogous to CPMG, called chemical exchange saturation transfer or CEST [18], was used and

measurement of the temperature dependence of the activation barrier between states revealed a very high barrier of 36 kcal/mol.

Finally, NMR has the capability of reporting directly on conformational entropy and it is now becoming clear that dynamic allostery is strongly related to changes in conformational entropy. One of the first examples of this phenomenon was in the catabolite activator protein (CAP) which displays strong negative cooperativity towards cyclic adenosine monophosphate (cAMP) binding. Kalodimos’ group showed that when cAMP binds to one subunit, the μ s-ms time scale motions increase in the associated subunit causing a larger entropy cost for binding the second cAMP [19]. Remarkably, although the motions changed in the second subunit, no changes in chemical shift were observed indicating that the structural ensemble of the second subunit wasn’t affected by the allostery, only the dynamics of the second subunit were affected when cAMP bound to the first subunit.

Amide hydrogen-deuterium exchange reveals allostery

As with NMR, there are too many publications to count in which HDX-MS reveals allostery, and this review will focus on a few salient examples. In an HDX-MS experiment, proteins are diluted into deuterated buffer (here $^2\text{H}_2\text{O}$ will be designated D_2O) and the exchange of amide hydrogens with deuterium is monitored over time using mass spectrometry after protease (typically pepsin) digestion. HDX-MS experiments monitor whether or not an NH group can exchange its proton. Proton exchange is a very different property from the nuclear chemical shift which is monitored by NMR. As such, NMR and HDX-MS give complementary information about allostery. Often, dynamic regions of a protein will exchange within minutes, and if their dynamic motions allow them to sample many conformational states, these NH groups will not be observed in the NMR experiment. Here we will try to compare and contrast the data obtained on a few proteins which have been studied both by HDX-MS and NMR in order to understand how the two experimental approaches differ. We note that NMR requires isotopic labeling of proteins, which requires heterologous expression that is not always feasible; it typically requires approx. 1 mg of protein dissolved at a concentration of 200 μM .

Interpretation of NMR data requires resonance assignments and as protein systems get larger this becomes something only experts can accomplish. HDX-MS does not require labeling during protein expression, it requires much less protein, typically a few hundred microliters of a 5 μM solution, and larger proteins and protein complexes are not a problem for the mass spectrometer to deconvolve.

Detection of allostery requires the study of a protein-ligand complex. We first showed in 1998 that when a ligand binds to a protein there can be local decreases in amide exchange that are due to the decreased solvent accessibility of surface amides (which may or may not be participating in H-bonds to other protein groups) [20]. In addition, both increases and decreases in amide exchange may be observed away from the ligand binding site that are due to changes in dynamics, *i.e.* rebalancing of the ensemble of states (several examples of this phenomenon will be described below). Before discussing the observation of allostery, one important issue must be dealt with, which is how to set-up the experiment. In HDX-MS analysis, the kinetics are traditionally described by Equation (1) where k_{ch} is the chemical exchange rate for the NH in question – values of which have been tabulated [21] and can be calculated using a program such as SPHERE (<https://protocol.fccc.edu/research/labs/roder/sphere/>) [22]. Allostery involves a protein-ligand interaction, and then there are two equilibria, the protein-ligand equilibrium and the equilibrium of the conformations which may or may not exchange (traditionally denoted as P_{cl} for closed or not exchanging or P_{op} for open conformations that can exchange) (Equation (2)).



In order for the HDX-MS experiment to be interpretable, the K_{D} of the ligand must be known and the quadratic binding equation must be used to determine how to shift the equilibrium towards $LP_{\text{cl}}\text{-H}$ so that essentially the only species being sampled in the HDX-MS experiment is LP [23]. This is not trivial since today's experiments typically dilute a 5 μM protein-ligand sample 10-fold resulting

in a 0.5 μM sample during the deuteration. While not intuitively obvious, even a K_{D} of 5 nM of ligand for protein will be only 90% bound if they are present at a 1:1 ratio. A 2:1 ratio of ligand:protein suffices to achieve 99% bound in this situation, but over time the ligand and protein will dissociate resulting in substantial amounts of protein (~50%) in the unbound conformation if deuteration is carried out for longer than 10 min. It is also important to note that interface protection will occur immediately, at the earliest timepoint, and will not build-up over time. Therefore, the informative time window for deuterium exchange in order to observe allostery is between 0 and 10 min. Note that when the ligand is at an appropriate concentration to achieve >99% bound, then Equation (2) reduces to Equation (1) and only the $LP_{\text{cl}}\text{-H}$ state need be considered in the HDX reaction.

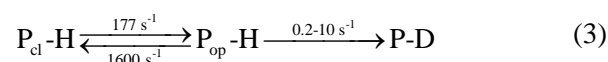
Kinases were one of the first protein classes to be analyzed by hydrogen-deuterium exchange mass spectrometry (HDX-MS) [20, 24]. Both HDX-MS and NMR have been extensively used to probe allostery in protein kinase A (PKA). HDX-MS showed that the N-terminal small lobe is dynamic and highly exchanging in the apo state of the kinase. Binding of ATP decreased exchange throughout the N-terminal lobe and in regions of the C-terminal lobe previewing the later NMR results. HDX-MS analysis of the PKA Tyr204Ala mutant revealed that this mutation alters the dynamics of the kinase and disrupts the allosteric network that connects substrate binding to catalysis. Wild type (WT) PKA and the Tyr204Ala mutant have also been studied extensively by NMR which revealed synchronous motions of the N-terminal lobe of PKA, which are responsible for nucleotide binding and release, and are desynchronized by the Tyr204Ala mutation, rendering the mutant enzyme catalytically inefficient [25]. Recent NMR experiments using methyl group motions allows for quantitative measurements of conformational entropy [26], and use of this method allowed for the analysis of the changes in conformational entropy. These experiments revealed positive cooperativity for substrate and nucleotide binding and negative cooperativity for ADP and phosphosubstrate binding [27]. HDX-MS has also contributed a large body of information on how the regulatory subunits of PKA engage and inhibit the catalytic subunit [28, 29].

Abl kinase has also been extensively studied by HDX-MS [30]. The HDX-MS work also revealed several different states of Abl kinase but focused more on the full-length (containing an SH2 and SH3 domain as well as the kinase domain) and C-terminally myristylated protein [31], which also stabilizes some states over others. This is the case for the A-loop and nearby residues of the α C helix in the Abl kinase. The A-loop is a critical region of kinases because it contains the DFG motif, which forms the docking site for substrate binding, as well as the tyrosine residue(s) that needs to be phosphorylated for activation. HDX-MS reports on this loop and its conformational changes much more readily than NMR, and the many states adopted by this region of the Abl kinase were, indeed, observed [30]. In the NMR work cited above, Xie *et al.* were able to observe these regions of the Abl kinase by decreasing the temperature of their NMR experiments. By collecting chemical shift information on many inhibited states as well as measuring through-space NOEs the structures of the various states could be solved. While HDX-MS reveals dynamic changes, attempts to use amide exchange information to predict structure have not been very successful.

Finally, our lab has extensively studied thrombin by both HDX-MS and NMR. Allosteric regulation of thrombin is provided by the protein cofactor thrombomodulin (TM), which converts the catalytic activity of thrombin away from fibrinogen and towards protein C instead, effectively switching thrombin from pro-coagulant to anticoagulant activity. As with the kinases, HDX-MS and NMR have provided complementary results. In addition, knowledge of the timescale of the dynamics from NMR as well as enhanced sampling accelerated molecular dynamics (aMD) simulations have provided insights into what is actually being observed in the HDX-MS experiments. TM interacts with thrombin with rapid kinetics ($k_a = 2 \times 10^7 \text{ M}^{-1}\text{s}^{-1}$, $k_d = 0.037 \text{ s}^{-1}$) and a K_D of 2 nM [32]. HDX-MS revealed that TM caused decreased exchange at anion binding exosite 1, the known allosteric regulatory binding site on thrombin [23]. In addition, several active site loops showed decreased exchange even though they were far from the TM binding site and could not be in contact with TM [33]. NMR relaxation dispersion

experiments allowed us to measure the kinetics of visitation to a higher energy “invisible state” in apo thrombin. In our work on thrombin, we measured a minor population of $4.1 \pm 6\%$ and the exchange rate, $k_{\text{ex}} = 1770 \text{ s}^{-1} \pm 60 \text{ s}^{-1}$. The measured exchange rate, k_{ex} , is the sum of the forward and reverse rates for the conformational transitions between the ground state ($\sim 95\%$) and the excited state ($\sim 5\%$); so k_{ex} represents a transition rate of $\sim 1/1600 \text{ s}^{-1}$ or a transition time from excited state to ground state of $\sim 600 \mu\text{s}$ and a transition rate of $1/177 \text{ s}^{-1}$ or a transition time from ground state to excited state of $\sim 6 \text{ ms}$ [34]. We recently studied the thrombin-TM complex by NMR as well, and TM completely rearranges which residues in thrombin are moving on the μs -ms time scale, but there are nearly an equivalent number of backbone NH groups that are moving in both apo thrombin and thrombin bound to TM (Peacock *et al.*, submitted). Although we could not extract a single transition rate, CPMG experiments measure motions in the μs -ms time regime and therefore the timescale of motions in the thrombin-TM complex must be similar.

Can the rate of exchange to the lowest populated “invisible” state be related to the rate of amide exchange? This is an interesting question because in allostery, ligand binding is shifting the equilibrium between states that should be energetically accessible (cf. Figure 1); ~ 2 - 10 kcal/mol higher in energy than the ground state. Let’s assume that the “open” state in the HDX-MS experiment is that energetically accessible state that is also observed by NMR. In that case, we can assign rates to the equilibrium in Equation (1). The range of chemical exchange rates for the amides in thrombin is $0.2 - 10 \text{ s}^{-1}$ at $25 \text{ }^\circ\text{C}$ and pH 6.5 (SPHERE (<https://protocol.fccc.edu/research/labs/roder/sphere/>) [22]. Equation (3) thus expresses the HDX reaction in terms of rates, which can be rearranged to solve for the exchange rate, k_{ex} according to Equation (4).



$$k_{\text{ex}} = \frac{k_{\text{op}}k_{\text{ch}}}{k_{\text{op}} + k_{\text{cl}} + k_{\text{c}}} \quad (4)$$

We can then solve for k_{ex} for the two limits of k_{ch} to solve for the range of exchange rates we can expect to be observing in the HDX experiment. For a k_{ch} of 0.2 s^{-1} , k_{ex} is 0.02 s^{-1} and for a k_{ch} of 10 s^{-1} , k_{ex} is 1 s^{-1} . These exchange rates in minutes are $1.2 - 60 \text{ min}^{-1}$. Translating these exchange rates into half-life yields $0.58 - 0.11 \text{ min}$ indicating that half of the amides will exchange within 0.1 to 0.5 min and 5 half-lives will occur within 0.5-3 min. Thus, in order to be sure to sample exchange to the lowest accessible higher energy states, the time window that should be sampled for HDX-MS is 0.1 to 5 min. This is exactly the time window in which changes in thrombin HDX due to TM binding is observed [35]. Note that the equation for k_{ex} is dominated by the ratio of the opening and closing rates and therefore by the ground state populations of the closed and open states. Since allostery requires an energetically accessible higher energy state, the exchange between states is expected to occur with an exchange rate in the μs -ms time regime, explaining why CPMG and/or CEST is the NMR experiment of choice. Similarly, if the allosteric change involves transitions from a closed, exchange inaccessible state to an open, exchange accessible state, then the time window in which amide exchange will reveal allostery is 0 - 10 min. Although an exhaustive search is impossible, we point the readers to several other reports of allostery observed by HDX-MS and note that the maximal difference in exchange between the ligand-bound state and the apo state is always manifested in the first 10 min of deuterium exchange [36-42].

The idea that motions in the μs -ms timescale are responsible for observations of differences in exchange was tested by comparing predictions from aMD simulations of thrombin and a single site mutant of thrombin, Trp215Ala, with HDX-MS data collected in this “fast-limit” time regime of 0 - 10 min. The enhanced sampling approach of aMD allows much more extensive exploration of the energy landscape to states that are separated by larger barriers such as states A and B in Figure 1. The simulations, which accounted for approximately 1 ms of motion were analyzed for H-bonding and solvent accessibility and then differences in these parameters were determined for the wild type

thrombin and the mutant. The experimental HDX-MS differences and the simulation results accurately predicted the allosteric changes upon mutation when *both* H-bonding and solvent accessibility were accounted for [43].

It is important to note that whereas NMR chemical shift changes typically report on the pathway of allostery from one site to another, NMR can miss the endpoints, particularly if they are dynamic surface loops which adopt a range of conformations and have an ensemble of chemical shifts that are then not observed. In contrast, it is unlikely that the H-bonding state of the pathway residues (recall that these are minimally frustrated and well-folded regions of the protein) will change and so HDX-MS typically reveals the endpoints of the allosteric pathway because it captures the changes in H-bonding and solvent accessibility of the loops at the ends of the pathway. Harkening back to the Newton’s Cradle example, then, we see that NMR reports on the middle balls whereas HDX-MS reports on the two balls at either end of the device.

HDX-MS has the capability of revealing allostery in systems that are not amenable to NMR spectroscopy. In the last few years, complexes such as E3 ligases that contain upwards of 10 different proteins have been analyzed by HDX-MS revealing that allostery can be transmitted through several proteins into others far away in the complex (Figure 5) [44, 45]. Allostery was also observed in AAA+ complexes [46] and even in whole viruses [47]. Finally, HDX-MS can also reveal allostery in membrane proteins [48].

We have been discussing situations in which the alternative conformation is a minor component and/or its deuterium exchange differs by 1-2 deuterons from the major state. These situations result in normally distributed mass envelopes that monotonically increase in mass over time of deuteration. HDX-MS can uniquely also identify alternative conformations which are major components of the ensemble, differ by at least 3 deuterons, and exchange on the minutes timescale. These states, which are said to be in EX1 exchange, show up as bimodal mass envelopes in which the less deuterated state eventually catches up with the more highly deuterated state over some minutes. A very interesting example of this was seen in P-glycoprotein. In one study, two different lipid

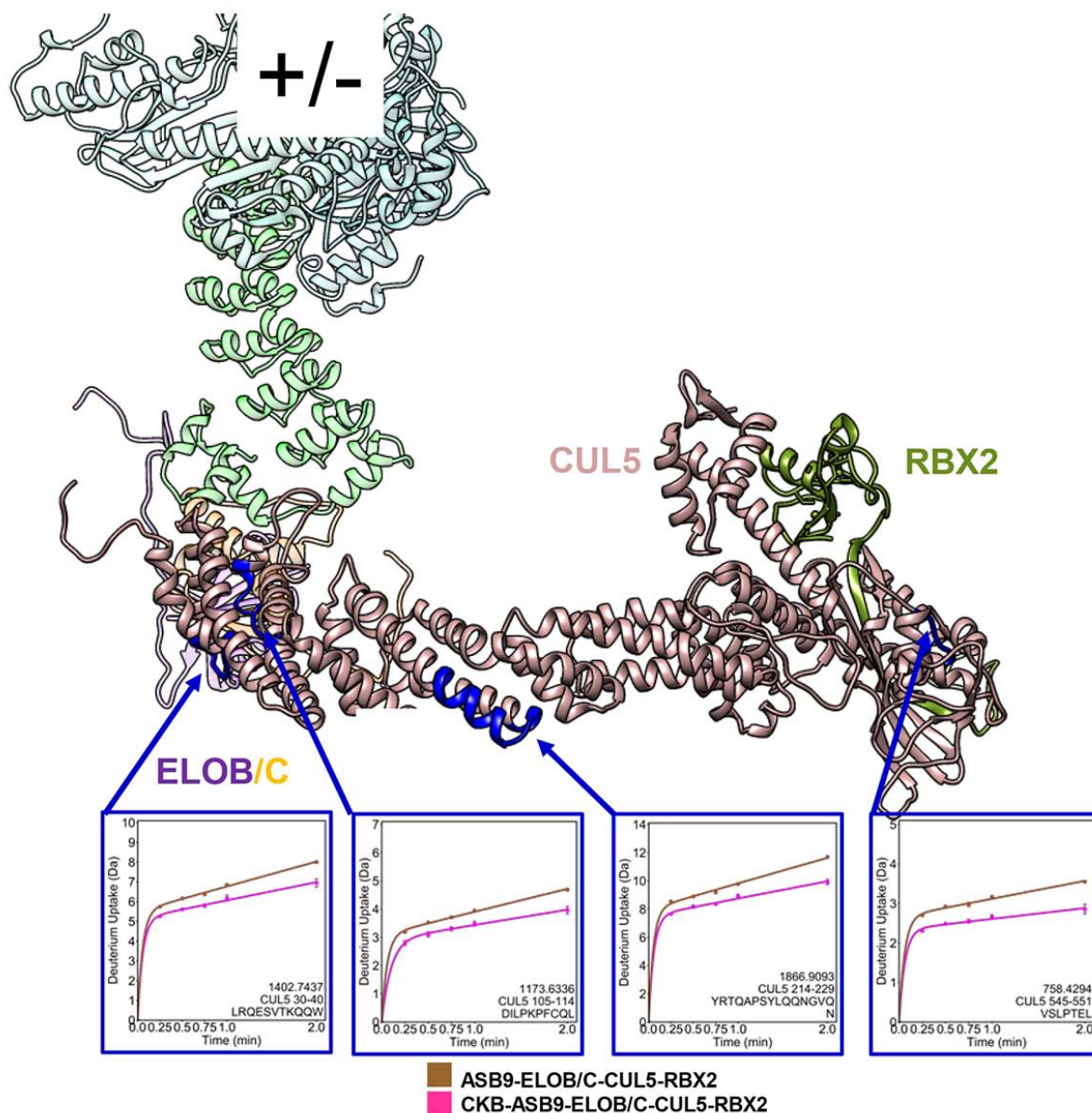


Figure 5. Long-range allostery in the cullin 5 ubiquitin E3 ligase induced by substrate (creatine kinase) binding (marked by the +/-) is observed as decreased exchange in specific regions of the cullin molecule extending to the RBX2 protein that holds the E2 subunit.

environments were compared and EX1 kinetics (*i.e.* motions that are slow enough to show two separate deuteration envelopes that convert to the more deuterated species over time) were observed in the more rigid nanodisc environment, but much of the “EX1 behavior” was lost when the protein was embedded in more flexible detergent micelles [49]. We also studied P-glycoprotein in detergent micelles and did not observe significant EX1 behavior. Remarkably, we were able to demonstrate

long-range allostery from the intracellular nucleotide binding domains through the transmembrane region to the extracellular domain [50].

As new methodologies developed, our conception of the thermodynamic mechanisms that drive allostery has also evolved, making it necessary to expand beyond the models originally constructed to describe the structural changes observed. NMR and HDX-MS experiments are unique in their

abilities to experimentally report on the conformational fluctuations relevant to protein allostery. Despite this similarity, the chemical phenomena measured by these two techniques are fundamentally distinct, and therefore their information content overlaps but is also complementary. Thus, the advancements being made in both the fields of NMR and HDX-MS enable allostery to be described in numerous protein systems that would not otherwise fit the traditional models, revealing multiple ways for modulation of energy landscapes of proteins and protein complexes to elicit diverse functions and regulatory mechanisms.

ACKNOWLEDGEMENTS

This work was supported by NIH grants R01HL127041 and S10 OD016234 and NSF grant MCB 1817774.

CONFLICT OF INTEREST STATEMENT

The authors declare no competing interests.

REFERENCES

1. Monod, J., Wyman, J. and Changeux, J. P. 1965, *J. Mol. Biol.*, 12, 88.
2. Koshland, D. E., Némethy, G. and Filmer, D. 1966, *Biochemistry*, 5, 365.
3. Hilser, V. J., Wrabl, J. O. and Motlagh, H. N. 2012, *Ann. Rev. Biophys.*, 41, 585.
4. Weinkam, P., Pons, J. and Sali, A. 2012, *Proc. Natl. Acad. Sci. USA*, 109, 4875.
5. Tsai, C.-J. and Nussinov, R. 2014, *PLoS Comput. Biol.*, 10, e1003394.
6. Ferreiro, D. U., Hegler, J. A., Komives, E. A. and Wolynes, P. G. 2011, *Proc. Natl. Acad. Sci. USA*, 108, 3499.
7. Ghode, A., Gross, L. Z. F., Tee, W. V., Guarnera, E., Berezovsky, I. N., Biondi, R. M. and Anand, G. S. 2020, *Biophys. J.*, 119, 1833.
8. Stivers, J. T., Abeygunawardana, C. and Mildvan, A. S. 1996, *Biochemistry*, 35, 16036.
9. Fuglestad, B., Gasper, P. M., Tonelli, M., McCammon, J. A., Markwick, P. R. L. and Komives, E. A. 2012, *Biophys. J.*, 103, 1.
10. Fuglestad, B., Gasper, P. M., McCammon, J. A., Markwick, P. R. and Komives, E. A. 2013, *J. Phys. Chem. B*, 117, 12857.
11. Palmer, A. G. R. 2014, *J. Magn. Reson.*, 241, 3.
12. Farber, P. J. and Mittermaier, A. 2015, *Biophys. Rev.*, 7, 191.
13. Palmer, A. G. R. and Koss, H. 2019, *Methods Enzymol.*, 615, 177.
14. East, K. W., Skeens, E., Cui, J. Y., Belato, H. B., Mitchell, B., Hsu, R., Batista, V. S., Palermo, G. and Lisi, G. P. 2020, *Biophys. Rev.*, 12, 155.
15. Velyvis, A., Yang, Y. R., Schachman, H. K. and Kay, L. E. 2007, *Proc. Natl. Acad. Sci. USA*, 104, 8815.
16. Byun, J. A., VanSchouwen, B. Akimoto, M. and Melacini, G. J. 2020, *Comput. Struct. Biotechnol.*, 18, 3803.
17. Xie, T., Saleh, T., Rossi, P. and Kalodimos, C. G. 2020, *Science*, 370, eabc2754.
18. Rennella, E., Huang, R., Velyvis, A. and Kay, L. E. 2015, *J. Biol. NMR*, 63, 187.
19. Popovych, N., Tzeng, S. R., Tonelli, M., Ebright, R. H. and Kalodimos, C. G. 2009, *Proc. Natl. Acad. Sci. USA*, 106, 6927.
20. Mandell, J. G., Falick, A. M. and Komives, E. A. 1998, *Proc. Natl. Acad. Sci. USA*, 95, 14705.
21. Bai, Y., Milne, J. S., Mayne, L. and Englander, S. W. 1993, *Proteins*, 17, 75.
22. Zhang, Y. Z., Paterson, Y. and Roder, H. 1995, *Protein Sci.*, 4, 804.
23. Mandell, J. G., Baerga-Ortiz, A., Akashi, S., Takio, K. and Komives, E. A. 2001, *J. Mol. Biol.*, 306, 575.
24. Hoofnagle, A. N., Resing, K. A., Goldsmith, E. J., and Ahn, N. G. 2001, *Proc. Natl. Acad. Sci. USA*, 98, 956.
25. Srivastava, A. K., McDonald, L. R., Cembran, A., Kim, J., Masterson, L. R., McClendon, C. L., Taylor, S. S. and Veglia, G. 2014, *Structure*, 22, 1735.
26. Kasinath, V., Sharp, K. A. and Wand, A. J. 2013, *J. Am. Chem. Soc.*, 135, 15092.
27. Wang, Y., Manu, V. S., Kim, J., Li, G., Ahuja, L. G., Aoto, P., Taylor, S. S. and Veglia, G. 2019, *Nat. Commun.*, 10, 799.
28. Anand, G. S., Hotchko, M., Brown, S. H., Ten Eyck, L. F., Komives, E. A. and Taylor, S. S. 2007, *J. Mol. Biol.*, 374, 487.
29. Badireddy, S., Yunfeng, G., Ritchie, M., Akamine, P., Wu, J., Kim, C. W., Taylor, S. S., Qingsong, L., Swaminathan, K. and Anand, G. S. 2011, *Mol. Cell. Proteomics.*, 10, M110.004390.

30. Panjarian, S., Iacob, R. E., Chen, S., Engen, J. R. and Smithgall, T. E. 2013, *J. Biol. Chem.*, 288, 5443.
31. Iacob, R. E., Zhang, J., Gray, N. S. and Engen, J. R. 2011, *PLoS One*, 6, e15929.
32. Baerga-Ortiz, A., Bergqvist, S. P., Mandell, J. G. and Komives, E. A. 2004, *Prot. Sci.*, 13, 166.
33. Fuentes-Prior, P., Iwanaga, Y., Huber, R., Pagila, R., Rumennik, G., Seto, M., Morser, J., Light, D. R. and Bode, W. 2000, *Nature*, 404, 518.
34. Handley, L. D., Fuglestad, B., Stearns, K., Tonelli, M., Fenwick, R. B., Markwick, P. R. L. and Komives, E. A. 2017, *Sci. Rep.*, 39575.
35. Handley, L. D., Treuheit, N. A., Venkatesh, V. J. and Komives, E. A. 2015, *Biochemistry*, 54, 6650.
36. Deredge, D., Li, J., Johnson, K. A. and Wintrode, P. L. 2016, *J. Biol. Chem.*, 291, 10078.
37. Deredge, D. J., Huang, W., Hui, C., Matsumura, H., Yue, Z., Moënne-Loccoz, P., Shen, J., Wintrode, P. L. and Wilks, A. 2017, *Proc. Natl. Acad. Sci. USA*, 114, 3421.
38. Ghosh, M., Wang, L. C., Ramesh, R., Morgan, L. K., Kenney, L. J. and Anand, G. S. 2017, *Biophys. J.*, 112, 643.
39. Ramsey, K. M., Dembinski, H. E., Chen, W., Ricci, C. G. and Komives, E. A. 2017, *J. Mol. Biol.*, 429, 999.
40. Kromann-Hansen, T., Lange, E. L., Sørensen, H. P., Hassanzadeh-Ghassabeh, G., Huang, M., Jensen, J. K., Muyldermans, S., Declerck, P. J., Komives, E. A. and Andreasen, P. A. 2017, *Sci. Rep.*, 7, 3385.
41. Lučić, I., Rathinaswamy, M. K., Truebestein, L., Hamelin, D. J., Burke, J. E., and Leonard, T. A. 2018, *Proc. Natl. Acad. Sci. USA*, 115, E3940.
42. Amatya, N., Wales, T. E., Kwon, A., Yeung, W., Joseph, R. E., Fulton, D. B., Kannan, N., Engen, J. R. and Andreotti, A. H. 2019, *Proc. Natl. Acad. Sci. USA*, 116, 21539.
43. Markwick, P. R. L., Peacock, R. B. and Komives, E. A. 2019, *Biophys. J.*, 116, 49.
44. Faull, S. V., Lau, A. M. C., Martens, C., Ahdash, Z., Hansen, K., Yebenes, H., Schmidt, C., Beuron, F., Cronin, N. B., Morris, E. P. and Politis, A. 2019, *Nat. Commun.*, 10, 3814.
45. Lumpkin, R. J., Baker, R. W., Leschziner, A. E. and Komives, E. A. 2020, *Nat. Commun.*, 11, 2866.
46. Bhat, J. Y., Miličić, G., Thieulin-Pardo, G., Bracher, A., Maxwell, A., Ciniawsky, S., Mueller-Cajar, O., Engen, J. R., Hartl, F. U., Wendler, P. and Hayer-Hartl, M. 2017, *Mol. Cell*, 67, 744.
47. Lim, X. X., Chandramohan, A., Lim, X. E., Crowe, J. E. J., Lok, S. M. and Anand, G. S. 2017, *Structure*, 25, 1391.
48. Pirrone, G. F., Emert-Sedlak, L. A., Wales, T. E., Smithgall, T. E., Kent, M. S. and Engen, J. R. 2015, *Anal. Chem.*, 87, 7030.
49. Li, M. J., Guttman, M. and Atkins, W.M. 2018, *J. Biol. Chem.*, 293, 6297.
50. Kopcho, N., Chang, G. and Komives, E. A. 2019, *Sci. Rep.*, 9, 15092.